J. Fluid Mech. (1986), *vol.* 172, *pp.* 183–209
Printed in Great Britain

Diffusion from a continuous source near a surface in steady reversing shear flow

By C. TURFUS

Department of Applied Mathematics and Theoretical Physics, University of Cambridge, Silver Street, Cambridge CB3 9EW

(Received 25 June 1985 and in revised form 28 November 1985)

The dispersion of continuous emissions from a line-source in a reversed-flow layer is analysed by means of diffusion equations; a family of exact solutions is found in the form of infinite series and/or integrals. It is shown that the concentration within the layer decays exponentially with the streamwise distance in the direction of reversed flow. The ground-level concentration near the source is found to be governed largely by the local mean flow; the value of the diffusivity affects the position of the maximum of ground-level concentration, but has little influence upon its magnitude. A useful upper limit is deduced for the background concentration due to recirculation effects. Further, a simple formula is given for the maximum value of the ground-level concentration for cases where the source is not too near the ground. The predictions for ground-level concentration are validated against experimental data for the particular case of a line source in the recirculating wake behind a two-dimensional backward-facing step. The extension of the analysis to the case of a point source is also discussed.

1. Introduction

It is well known (Taylor 1953) that the incorporation of shear into the mean-flow profile in a diffusion problem can have radical effects upon the concentration field established. Taylor's (1953) original calculation demonstrated this, in the context of turbulent pipe flow, by an asymptotic analysis. Several exact solutions have since been found for related situations. For example, the problem of an instantaneous point release into an unbounded uniform shear flow is solved (among others) by Elrick (1962). Solutions for a continuous source obtained by integrating the Elrick (1962) solution, are presented by Okubo & Karweit (1969). All these solutions show the characteristic 'stretching' of the puffs or plumes in the streamwise direction.

For the case of a unidirectional shear flow near a non-absorbing surface, Smith (1957) and Kay (1985) have presented whole families of solutions which illustrate the strong influence of the mean shear in determining, for example, the position and magnitude of the maximum ground-level concentration.

An interesting problem emerges when we extend the problem of Smith (1957) to the case of a steady *reversing* shear-flow, for in such a case the source is not releasing contaminant into clean ambient fluid but into fluid containing recirculated contaminant. It is on this case that our attention will be focused in the present paper.

The type of fluid-flow configuration we have in mind (see figure 1) is that of a boundary layer with a reversed-flow layer immediately adjacent to the boundary. It is one which arises in a large number of environmental and industrial contexts. Some environmental applications are the flow in the recirculating wake behind a

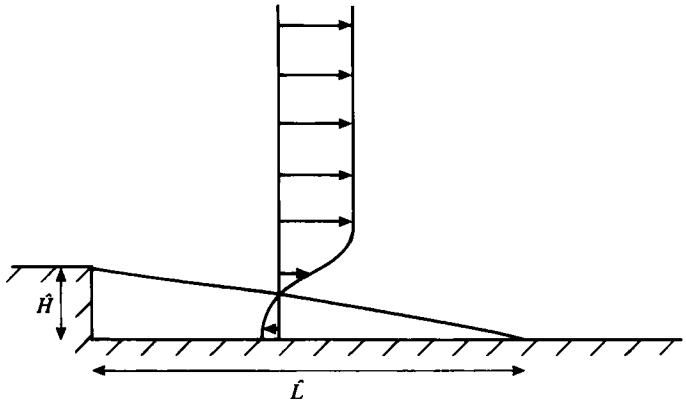

FIGURE 1. Definition sketch for reversing flow near a boundary.

fence, steep hill or wide building, the sea-breeze problem where a buoyancy-driven cold layer of sea-air can flow inland against an adverse mean flow above, and the situation where an estuarine flow separates from the bank downstream of a sharp bend; on a larger scale there is also the density-driven exchange between saline and fresh water in the world's oceans. Examples of industrial applications are convective flow in a furnace or heated tank, confined jets in combustion chambers and flows in mixing vessels driven either mechanically or by bubble rise.

In many of these situations it is of importance to understand the mechanism of dispersion as well as the flow details. For example, in the case of the flow in the recirculating wake behind a building or structure, it is known (Wilson & Britter 1982) that the highest building-surface concentrations result from situating a source of contaminant within the recirculating region; a predictive theory thus appears desirable for such situations.

We consider here the particular problem of a continuously emitting line-source located within the reversed-flow layer. We shall use a diffusion equation analysis, to suggest what kind of answers should be given to the following questions, concerning the concentration field established:

(i) What and where is the maximum surface concentration, and how much influence does the source position have upon our conclusions?

(ii) How much contaminant is recirculated and is there an upper limit to this effect?

(iii) Is it essential to model the *global* mean-flow details?

(iv) How sensitive is the mean concentration distribution to the turbulence levels?

In response to the third of these questions, it obviously is important to model the global mean flow if this is strongly two- or three-dimensional. But if, as we have suggested in figure 1, the streamwise lengthscale $\hat{L}$ of the mean velocity field is much greater than the corresponding lengthscale, $\hat{H}$, normal to the surface, it is possible that a model incorporating only *horizontal* mean motion will be adequate for some purposes. More specifically, if the plume from the source fills the reversed layer before the horizontal (or vertical) mean velocity changes substantially, and if the vertical mean velocity is small, then we may be justified in ignoring the vertical mean motions. Throughout our analysis we shall suppose such a slow horizontal variation, expressed mathematically by the condition $\kappa_e \hat{L}/U_0 \gg \hat{H}^2$, where U_0 is a typical backflow velocity and κ_e is an effective turbulent diffusivity. By assuming that the answer to (iii) is negative, we propose a model with purely streamwise mean flow. This allows

analytical solutions to be found for the diffusion equation, which can then be used to suggest answers to questions (i), (ii) and (iv). The validity of our approach is tested by comparing predicted ground-level concentrations with data from a wind-tunnel experiment carried out for a porous line-source positioned in the recirculating wake behind a backward-facing step (unpublished observations of Quante & Etheridge documented by Turfus 1985).

The diffusion-equation solution procedure is described in §2, the main conclusions of which are expressed in equations (2.12), (2.16) and (2.21). These solutions are used to investigate the sensitivity of the mean concentration field to the various flow parameters in §§3 and 4. In §5, the extension of the analysis to point sources is discussed and some of the associated difficulties pointed out. Finally, §6 draws together some conclusions.

2. Diffusion equation solution

In attempting to model dispersion in a recirculating flow by diffusion-equation analysis, we shall be relying on two basic assumptions:

(i) that the gradient-flux relation holds, i.e.

$$\overline{u_i \hat{C}} = \overline{u_i}\,\overline{\hat{C}} + \kappa_{ij} \frac{\partial \overline{\hat{C}}}{\partial \hat{x}_j}, \tag{2.1}$$

where $u_i(\hat{\boldsymbol{x}}, t)$ is the ith component of the velocity of the fluid into which contaminant is released, $\hat{C}(\hat{\boldsymbol{x}}, t)$ is the instantaneous distribution of contaminant concentration resulting from an established line source, $\kappa_{ij}(\hat{\boldsymbol{x}})$ is the diffusivity tensor assumed to be dependent only on the statistical properties of $\boldsymbol{u}(\hat{\boldsymbol{x}}, t)$, and the overbar denotes ensemble averaging;†

(ii) the assumption, discussed above, that the mean vertical motions can be neglected in the centre of the wake, i.e. the answer to question (iii) in §1 is negative.

Neither of these assumptions can be strictly justified *a priori*. It has frequently been shown (see e.g. Corrsin 1974) that the strict conditions for (i) to apply are virtually never satisfied in practical applications. Nevertheless useful results are frequently found. We thus proceed by supposing that (i) and (ii) are not inappropriate, then test our assumptions *a posteriori* by comparison of the results obtained with experimental data. It will be seen that as far as ground-level concentrations are concerned our procedure appears to be validated.

Based on (2.1) a standard diffusion equation representation of the dispersion from a line-source strength Q at position $(\hat{x}_1, \hat{x}_3) = (0, -\hat{x}_{30})$ can be derived:

$$\overline{u}_i \frac{\partial \overline{\hat{C}}}{\partial \hat{x}_i} = \frac{\partial}{\partial \hat{x}_i}\left(\kappa_{ij} \frac{\partial \overline{\hat{C}}}{\partial \hat{x}_i}\right) + Q\delta(\hat{x}_1)\,\delta(\hat{x}_3 + \hat{x}_{30}). \tag{2.2}$$

With boundary conditions

$$\overline{\hat{C}} \to 0 \quad \text{as } (\hat{x}_1^2 + \hat{x}_3^2)^{\frac{1}{2}} \to \infty, \tag{2.3a}$$

and

$$\kappa_{3j} \frac{\partial \overline{\hat{C}}}{\partial \hat{x}_j} = 0 \quad \text{on the surface } \hat{x}_3 = -\hat{h}. \tag{2.3b}$$

Since we are considering a line source in a two-dimensional mean flow, we can ignore all spanwise ($\hat{x}_2$-) gradients. We make the further simplifications of assuming that

† It is further assumed that *all* functions are statistically stationary in time.

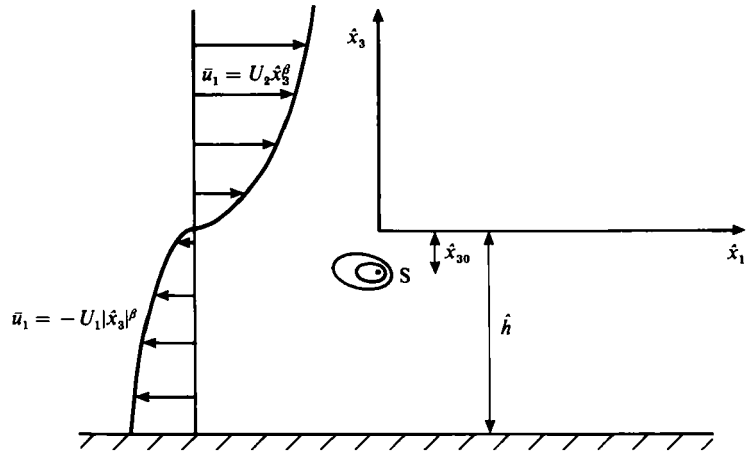

FIGURE 2. Definition sketch for general diffusion problems with power-law profiles.

$\bar{\boldsymbol{u}} = (\bar{u}_1(\hat{x}_3), 0, 0)$ and that $\kappa_{ij} = 0$, $i \neq j$ with $\kappa_{33} = \kappa$, a constant and $\kappa_{11} = \hat{\epsilon}\kappa$, where $\hat{\epsilon}$ also is a constant, in practice set equal to either 0 or 1. Equation (2.2) then becomes

$$\bar{u}_1(\hat{x}_3)\frac{\partial \bar{C}}{\partial \hat{x}_1} = \kappa\left(\hat{\epsilon}\frac{\partial^2 \bar{C}}{\partial \hat{x}_1^2} + \frac{\partial^2 \bar{C}}{\partial \hat{x}_3^2}\right) + Q\delta(\hat{x}_1)\,\delta(\hat{x}_3 + \hat{x}_{30}). \tag{2.4}$$

We assume the velocity profile $\bar{u}_1(\hat{x}_3)$ has a power-law form:

$$\begin{aligned} \bar{u}_1(\hat{x}_3) &= -U_1|\hat{x}_3|^\beta \quad (-\hat{h} \leqslant \hat{x}_3 \leqslant 0), \\ &= U_2\hat{x}_3^\beta \quad (\hat{x}_3 > 0), \end{aligned} \tag{2.5}$$

so flow reversal occurs at $\hat{x}_3 = 0$ and the reverse-flow layer has thickness $\hat{h}$ (see figure 2).

We introduce the following non-dimensionalization, in terms of a typical vertical lengthscale $\hat{H}$:

$$\hat{x}_3 = z\hat{H}; \quad \hat{x}_{30} = z_0\hat{H}; \quad \hat{h} = h\hat{H}; \quad \hat{x}_2 = y\hat{H};$$

$$\hat{x}_1 = \frac{xU_1\hat{H}^{2+\beta}}{\kappa}; \quad \bar{C} = \frac{CQ}{U_1\hat{H}^{1+\beta}}; \quad \hat{\epsilon} = \frac{\epsilon U_1^2\hat{H}^{2+2\beta}}{\kappa^2},$$

in terms of which (2.3)–(2.5) become

$$-|z|^\beta\frac{\partial C}{\partial x} - \epsilon\frac{\partial^2 C}{\partial x^2} - \frac{\partial^2 C}{\partial z^2} = \delta(x)\,\delta(z+z_0) \quad (-h \leqslant z \leqslant 0), \tag{2.6a}$$

$$\Gamma z^\beta\frac{\partial C}{\partial x} - \epsilon\frac{\partial^2 C}{\partial x^2} - \frac{\partial^2 C}{\partial z^2} = 0 \quad (z > 0), \tag{2.6b}$$

with

$$C \to 0 \quad \text{as } (x^2+z^2)^{\frac{1}{2}} \to \infty, \tag{2.7a}$$

$$\frac{\partial C}{\partial z} = 0 \quad \text{on } z = -h, \tag{2.7b}$$

where $\Gamma = U_2/U_1$.

The reader not interested in the mathematical details of the solution of this diffusion equation may omit the remainder of this section, the major results of which are expressed in (2.12), (2.16) and (2.21).

This problem as it stands is similar to those considered by Smith (1957) and Kay

(1985), except that in those cases there was no flow reversal. As it turns out, this reversal makes a critical difference to the solution procedure; the straightforward Laplace transform method adopted by these authors becomes inapplicable in our case. The reason for this is that the boundary condition at $x = 0$ required for the solutions in $x < 0$ and $x > 0$ is unknown. Ludford & Robertson (1973) encountered this same difficulty in dealing with a related problem. Their paper considers the diffusion of heat in a parallel reversing flow between two planes, the diffusion in their case being forced by a step-function distribution of temperature on one of the planes. They note that the problem could be solved by means of a full Fourier transform, but choose to solve it as two Laplace transform problems with unknown boundary condition at $x = 0$. By matching the two resultant solutions at $x = 0$, they are then able to calculate the unknown common boundary condition. This latter method, they explain, has broader application than the Fourier transform method. However, we shall in this instance adopt the former, more straightforward approach, taking a full Fourier transform of the concentration field:

$$\tilde{C}(k,z) = \frac{1}{2\pi}\int_{-\infty}^{\infty} C(x,z)\,\mathrm{e}^{-\mathrm{i}kx}\,\mathrm{d}x,$$

in terms of which (2.6) and (2.7) become

$$-|z|^{\beta}\,\mathrm{i}k\tilde{C} + \epsilon k^2\tilde{C} - \frac{\partial^2\tilde{C}}{\partial z^2} = \frac{\delta(z+z_0)}{2\pi} \quad (-h \leqslant z \leqslant 0), \tag{2.8a}$$

$$\Gamma z^{\beta}\,\mathrm{i}k\tilde{C} + \epsilon k^2\tilde{C} - \frac{\partial^2\tilde{C}}{\partial z^2} = 0 \quad (z > 0), \tag{2.8b}$$

with

$$\tilde{C} \to 0 \quad \text{as } z \to \infty, \tag{2.9a}$$

$$\frac{\partial\tilde{C}}{\partial z} = 0 \quad \text{on } z = -h. \tag{2.9b}$$

We shall deal separately with the cases $\beta = 0$ and $0 < \beta \leqslant 1$ because of the special simplifying features of the former, corresponding as it does to two uniform layers. For most purposes we shall set $\epsilon = 0$, but we shall illustrate, using the particular case $\beta = 1$, how a non-zero value can in general be incorporated.†

In solving the system (2.8) subject to (2.9), the k-plane is cut along the branch line $\arg k = \frac{1}{2}\pi$. We can then uniquely define a complex number

$$\xi = (\mathrm{i}k)^{\frac{1}{2}} = |k|^{\frac{1}{2}}\,\mathrm{e}^{\frac{1}{2}\mathrm{i}(\arg k + \frac{1}{2}\pi)}$$

which has the convenient property that $\mathrm{Re}\,\xi > 0$.

We consider first the case $\beta = 0$ for which we introduce the further notation $\Gamma = \tan^2\phi$. Putting $\epsilon = 0$ we can obtain a solution for $\tilde{C}(k,z)$ by standard Green function method:

$$\tilde{C}(k,z) = -\frac{\cos(-\xi z_0 + \phi)\cos(\xi(h+z))}{2\pi\xi\sin(\xi h - \phi)} \quad (-h \leqslant z < -z_0), \tag{2.10a}$$

$$= -\frac{\cos(\xi z + \phi)\cos(\xi(h-z_0))}{2\pi\xi\sin(\xi h - \phi)} \quad (-z_0 < z \leqslant 0), \tag{2.10b}$$

$$= -\frac{\exp(-\xi z\tan\phi)\cos(\xi(h-z_0))}{2\pi\xi\sin(\xi h - \phi)}\cos\phi \quad (z > 0), \tag{2.10c}$$

where the definition of ξ ensures that $\tilde{C} \to 0$ as $z \to \infty$.

† The setting of $\epsilon = 0$ is consistent with our previous assumption that $\kappa_e L/U_0 \gg \hat{H}^2$, for in such cases only vertical diffusion is important, with horizontal spread dominated by advection.

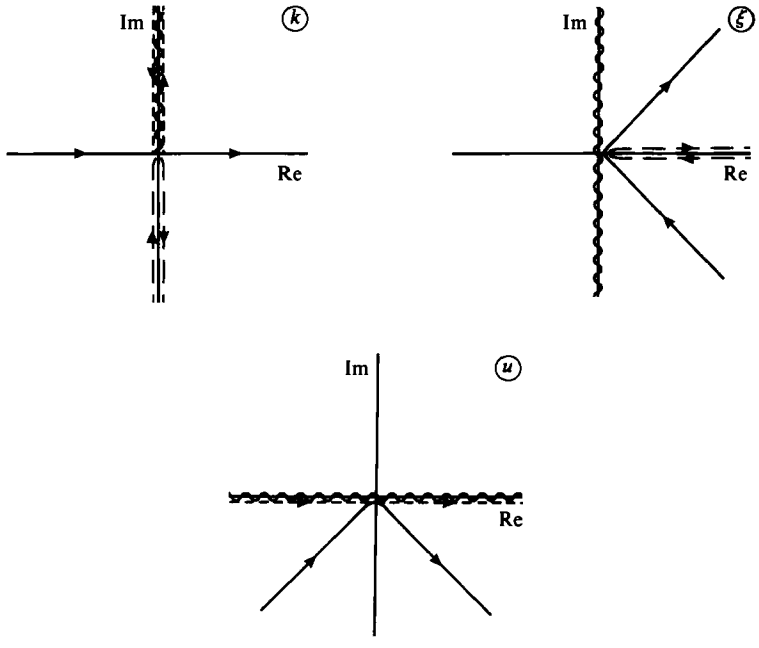

FIGURE 3. Contour manipulations in k-, ξ- and u-space. —►—, original contour;—►—, deformed contour for $x<0$ (C_1);--►--, deformed contour for $x>0$ (C_2); ∿∿, branch cut.

In order to inverse transform these expressions, we consider separately the regions $x<0$ and $x>0$. For the former case the inversion integral

$$C(x,z)=\int_{-\infty}^{\infty}\tilde{C}(k,z)\,\mathrm{e}^{\mathrm{i}kx}\,\mathrm{d}k, \tag{2.11}$$

can be written in terms of ξ as two integrals from '$\infty\,\mathrm{e}^{-\frac{1}{4}\mathrm{i}\pi}$' to 0 and from 0 to '$\infty\,\mathrm{e}^{\frac{1}{4}\mathrm{i}\pi}$'. We can by appeal to Cauchy's theorem replace these two integrals by a single integral along the contour C_1 depicted in figure 3 for the k-plane and the ξ-plane. (Note that all the poles of $\tilde{C}$ lie on the negative imaginary k-axis or positive real ξ-axis.) Thus, in terms of ξ:

$$C(x,z)=\frac{2}{\mathrm{i}}\int_{C_1}\tilde{C}(-\mathrm{i}\xi^2,z)\,\mathrm{e}^{\xi^2x}\,\xi\,\mathrm{d}\xi.$$

This integral can in turn be replaced, via Cauchy's residue theorem, by

$$C(x,z)=4\pi\sum_{n=0}^{\infty}\left\{\text{residue of }\xi\tilde{C}(-\mathrm{i}\xi^2,z)\quad\text{at }\lambda_n\right\}\mathrm{e}^{\lambda_n^2x},$$

with the summation evaluated over all the poles $\lambda_n=(n\pi+\phi)/h$ of $\xi\tilde{C}$.†

The solution is then:

$$C(x,z)=\frac{2}{h}\sum_{n=0}^{\infty}\cos\lambda_n(h-z_0)\cos\lambda_n(h+z)\,\mathrm{e}^{\lambda_n^2x}\quad(x<0;\ -h\leqslant z<-z_0). \tag{2.12a}$$

We note that by the reciprocal theorem of Smith (1957), the roles of z and the source height $-z_0$ can be interchanged to obtain a solution valid for $-z_0<z\leqslant 0$. In fact the solution, being symmetric, does not change, so we conclude (2.12a) is valid for $-h\leqslant z\leqslant 0$, as can be verified by direct computation from (2.10b).

† The minus sign appears because the poles are circumnavigated in a clockwise sense.

By similar means, (2.10*c*) can be shown to yield

$$C(x,z) = \frac{2}{h}\sum_{n=0}^{\infty} \cos\lambda_n(h-z_0)\cos\lambda_n h\, \mathrm{e}^{-\tan\phi\lambda_n z}\,\mathrm{e}^{\lambda_n^2 x} \quad (x<0;\, z>0). \quad (2.12b)$$

To solve for $x>0$ we use a contour manipulation similar to the one just described to turn the integral (2.11) into a real expression. The contour used is that denoted C_2 in figure 3. On C_2, ik is real and negative, so that the integrand again decays exponentially as $x\to\infty$. In terms of $u = \xi\,\mathrm{e}^{-\frac{1}{4}i\pi}$

$$C(x,z) = \int_{C_2} 2i\tilde{C}(iu^2,z)\,\mathrm{e}^{-u^2x}\,u\,\mathrm{d}u = 2i\int_{-\infty}^{\infty}\tilde{C}(iu^2,z)\,\mathrm{e}^{-u^2x}\,u\,\mathrm{d}u.$$

It can be seen that replacing u by $u\,\mathrm{e}^{i\pi}$ maps $\tilde{C}$ to $\tilde{C}^*$, where * denotes complex-conjugate. Hence

$$C(x,z) = \mathrm{Re}\int_0^{\infty} 4i\tilde{C}(iu^2,z)\,\mathrm{e}^{-u^2x}\,u\,\mathrm{d}u. \quad (2.13)$$

Considering first $-h\leqslant z<-z_0$, we note that (2.10*a*) can be expressed in terms of u as:

$$\tilde{C}(k,z) = \frac{\cosh(uz_0+i\phi)\cosh(u(h+z))}{2\pi u\sinh(uh+i\phi)}$$

$$= \frac{[\sinh(u(h+z_0))+\sinh(u(h-z_0))\cos 2\phi - i\cosh(u(h-z_0))\sin 2\phi]}{2\pi u(\cosh(2uh)-\cos 2\phi)}\cosh(u(h+z)),$$

and substituting into (2.13) and taking the real part:

$$C(x,z) = \frac{2}{\pi}\int_0^{\infty}\frac{\cosh(u(h-z_0))\cosh(u(h+z))\sin 2\phi\,\mathrm{e}^{-u^2x}}{\cosh(2uh)-\cos 2\phi}\mathrm{d}u \quad (x>0,\ -h\leqslant z\leqslant -z_0). \quad (2.14a)$$

Again, from symmetry we see that this result must hold for $-h\leqslant z\leqslant 0$. Finally from (2.10*c*) we have

$$C(x,z) = \frac{2}{\pi}\int_0^{\infty}[\cosh(uh)\cos(uz\tan\phi)\sin 2\phi + 2\sinh(uh)\sin(uz\tan\phi)\cos^2\phi] \times\frac{\cosh(u(h-z_0))\,\mathrm{e}^{-u^2x}}{\cosh(2uh)-\cos 2\phi}\mathrm{d}u \quad (x>0,\ z>0). \quad (2.14b)$$

Equations (2.12) and (2.14) together constitute a complete solution to the problem.

We note in conclusion that (2.14*a*) can be re-expressed as an infinite series which is useful for evaluations in the near field (small x), but which is also physically revealing concerning the structure of our solution. We show this by expanding the denominator as

$$[\cosh(2uh)-\cos 2\phi]^{-1} = 2\sum_{n=0}^{\infty}\mathrm{e}^{-2uh(n+1)}\sum_{r=0}^{[\frac{1}{2}n]}\binom{n-r}{r}(-)^r(2\cos 2\phi)^{n-2r}.$$

This allows us to expand the integrand (2.14*a*) as an infinite sum, each term of which can be analytically integrated. In terms of

$$f(x) := \mathrm{e}^{x^2}\,\mathrm{erfc}(|x|),$$

the result is

$$C(x,z) = \sum_{n=0}^{\infty} \sum_{r=0}^{[\frac{1}{2}n]} \binom{n-r}{r} (-)^r (2\cos 2\phi)^{n-2r} \sin 2\phi \times \frac{1}{(4\pi x)^{\frac{1}{2}}} \sum_{\substack{++\\+-\\-+\\--}} f\left(\frac{2(n+1)h \pm (h+z) \pm (h-z_0)}{(4x)^{\frac{1}{2}}}\right) \quad (x>0,\ -h \leqslant z \leqslant 0). \quad (2.15)$$

The solution takes the form of an infinite array of 'distributed' sources and sinks of contaminant, located above $z = 0$ or below $z = -h$; these are positioned regularly at heights

$$\begin{aligned} z_s &= -z_0 \pm 2(n+1)h \\ &= z_0 + 2nh \\ &= z_0 - 2(n+2)h. \end{aligned}$$

It is worth noting that *no* effective source term appears corresponding to the real source at $z = -z_0$: since our model has no horizontal diffusivity, contaminant cannot pass from the source directly to the region $x > 0$ but must first diffuse into the upper layer, be advected downstream, then diffuse down again. This constitutes an inadequacy of our model in this near-source region.

We consider further asymptotic analyses of the above solution in §4 and now turn our attention instead to the problem with general β. The details of the solution of this problem and the notation necessary to express the answer are a little involved so have been reproduced in the Appendix. Essentially the method is the same as that described for $\beta = 0$.

We do reproduce here, however, a particular form of the solution for the case $\beta = 1$; all cases of physical interest should have values of β between this value (corresponding to a linear shear) and the value $\beta = 0$ already discussed. The $\beta = 1$ solution has a particularly straightforward formulation in terms of the well-tabulated Airy functions, when $u_1 = u_2$ ($\Gamma = 1$).

If the zeros of the derivative of the Airy function $\mathrm{Ai}'(x)$ are $\{a_n'; n = 1, 2, \ldots\}$ then the solution can be written

$$C(x,z) = \frac{3}{h^2} \sum_{n=1}^{\infty} \frac{\mathrm{Ai}(-a_n' z_0/h)\,\mathrm{Ai}(z a_n'/h)}{\mathrm{Ai}(-a_n')^2} \mathrm{e}^{(a_n'/h)^3 x} \quad (x<0), \quad (2.16a)$$

$$= 3\int_0^{\infty} \frac{[\mathrm{Ai}(uz_0)\,\mathrm{Bi}'(uh) - \mathrm{Bi}(uz_0)\,\mathrm{Ai}'(uh)] \times [\mathrm{Ai}(-uz)\,\mathrm{Bi}'(uh) - \mathrm{Bi}(-uz)\,\mathrm{Ai}'(uh)]}{\mathrm{Ai}'(uh)^2 + \mathrm{Bi}'(uh)^2} \mathrm{e}^{-u^3 x} u\,\mathrm{d}u \quad (x>0). \quad (2.16b)$$

Because of the convenient form of this solution, we use it to illustrate how our solution procedure can be extended to incorporate streamwise diffusivity. Thus we shall solve the non-dimensional system

$$zC_x - \epsilon C_{xx} - C_{zz} = \delta(x)\,\delta(z+z_0), \quad (2.17)$$

with boundary conditions given by (2.7), where subscripts x, y and z are used to denote partial differentiation with respect to these variables. On Fourier transforming, (2.17) becomes

$$(\mathrm{i}zk + \epsilon k^2)\,\bar{C} - \bar{C}_{zz} = \frac{\delta(z+z_0)}{2\pi}. \quad (2.18)$$

The solution can be written in terms of the function

$$s(z) = (\mathrm{i}k)^{\frac{1}{3}}(z - \epsilon \mathrm{i}k) \tag{2.19}$$

(see Pedley 1980, p. 406), as

$$\tilde{C}(k,z) = \frac{\mathrm{Ai}(s(-z_0))}{2(\mathrm{i}k)^{\frac{1}{3}}} \left\{ \mathrm{Bi}(s(z)) - \frac{\mathrm{Bi}'(s(-h))}{\mathrm{Ai}'(s(+h))} \mathrm{Ai}(s(z)) \right\} \quad (-h \leqslant z < -z_0). \tag{2.20}$$

A symmetric result with $s(-z_0)$ exchanged with $s(z)$ holds for $z > -z_0$. As before we apply a branch cut to the k-plane at $\arg k = \frac{1}{2}\pi$, so that $|\arg(s)| < \frac{1}{3}\pi$ for $z > 0$ and $\tilde{C}(k,z) \to 0$ as $z \to \infty$. Using (2.20) in (2.11), distorting the k-integration onto C_1 as before and setting $t = (\mathrm{i}k)^{\frac{1}{3}}$, we obtain

$$\begin{aligned} C(x,z) &= 2\pi\mathrm{i} \sum_{\substack{\text{Residues} \\ \text{w.r.t. } t}} \frac{3t}{2\mathrm{i}} \mathrm{Ai}(t(z - \epsilon t^3)) \, \mathrm{Ai}(t(-z_0 - \epsilon t^3)) \, \mathrm{Bi}'(t(-h - \epsilon t^3)) \, \mathrm{e}^{t^3 x} \\ &= 3 \sum_{r=1}^{\infty} \frac{\mathrm{Ai}(-t_r(z_0 + \epsilon t_r^3)) \, \mathrm{Ai}(-t_r(-z + \epsilon t_r^3)) \, \mathrm{e}^{t_r^3 x}}{(h + \epsilon t_r^3)(h + 4\epsilon t_r^3) \, \mathrm{Ai}(-a_r')^2} \quad (x < 0), \end{aligned} \tag{2.21}$$

where the a_r' are as defined for equation (2.16a) and the t_r satisfy

$$(h + \epsilon t_r^3) t_r = a_r'.$$

A similar solution of the form of (2.16b) can be derived for $x > 0$ but is less useful than (2.21), so not quoted here.

3. Evaluation of results

In order to test the usefulness of our diffusion-equation model of wake dispersion, we carry out some evaluations of the formulae derived in §2, scaled so as to correspond as closely as possible with an experimental configuration for which data are available. The configuration we have in mind is that of a line source placed in the recirculating wake behind a two-dimensional backward-facing step at high Re. Quante & Etheridge (unpublished observations) have made measurements for such a situation where the line-source is positioned at 2.4 step heights downstream of the step and at a height of 0.4 step-heights above ground level. Their results for mean concentration are presented by Turfus (1985) in comparison with his numerical results, obtained by a trajectory simulation technique involving a discrete vortex model. Flow statistics were not measured by Quante & Etheridge, so we rely mainly upon the computed flow statistics of Turfus (1985) in the vicinity of the source to parameterize our diffusion-equation model. He found that the mean horizontal flow reversed at a height of about $0.5\hat{H}$, $\hat{H}$ being the step height (see figure 4) and reached a minimum of about $-0.2\ U_\infty$ at the ground, where U_∞ is the mean free-stream speed, far from the wall. The notation $\hat{H}$ has already been introduced (in the non-dimensionalization leading to (2.6)) to denote a vertical lengthscale for diffusion. We shall henceforth consider this 'vertical lengthscale' to be precisely the step height. In addition, he found a vertical velocity variance of $0.01\ U_\infty^2$ and Lagrangian timescale, T_{L}^{ww}, based on vertical velocity fluctuations, of $1.0\ \hat{H}/U_\infty$, for the source position, leading to the following estimate of vertical turbulent diffusivity:

$$\kappa_{\mathrm{e}} = \sigma_w^2 T_{\mathrm{L}}^{ww} \approx 0.01\ U_\infty \hat{H}.$$

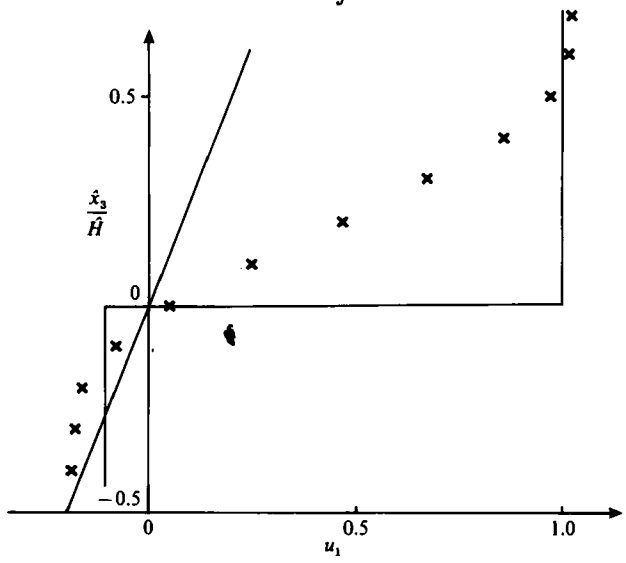

FIGURE 4. Horizontal mean velocity profile $\overline{u}_1(\hat{x}_3)$ at source position $|\Delta\hat{x}_1| = 2.5\,\hat{H}$ behind backward-facing step, compared with idealized profiles used in diffusion equation. ×, $\overline{u}_1(\hat{x}_3)$ from discrete vortex model; ——, idealized profiles used in the diffusion equation.

Thus we propose setting $\kappa = 0.01\,U_\infty \hat{H}$ in (2.4). As an approximation to the mean-flow profile $\overline{u}_1(\hat{x}_3)$ derived from the discrete vortex model of Turfus (1985), we consider two choices:

(i) $\beta = 0$; $U_1 = 0.1\,U_\infty$, $U_2 = U_\infty$ (a step profile),

(ii) $\beta = 1$; $U_1 = U_2 = \dfrac{0.4\,U_\infty}{\hat{H}}$ (a linear profile),

both shown in figure 4.

We further set $\hat{h} = 0.5\,\hat{H}$ and $\hat{x}_{30} = 0.1\,\hat{H}$, so that $h = 0.5$, $z_0 = 0.1$ in the non-dimensional notation.

For purposes of standardization we present all concentrations in the form $\chi(\hat{x}_1, \hat{x}_3) = \bar{C}U_\infty \hat{H}/Q$ and we use dimensional variables.

As an illustration of the form of our solution, we have calculated $\chi(\hat{x}_1, \hat{x}_3)$ for case (ii) with $\hat{\epsilon} = 0$ (no streamwise diffusivity). The result is shown in the form of concentration isopleths for $-2.0\,\hat{H} \leqslant \hat{x}_1 \leqslant 0$, $-0.5\,\hat{H} \leqslant \hat{x}_3 \leqslant 0.5\,\hat{H}$ in figure 5. It will be noted how the plume 'dips' as one moves leftwards from the source, due to contaminant being swept away to the right in the upper layer. However, *near* the surface, a tongue of contaminant can be seen stretching leftwards from the source, as a result of the recirculated contribution.

As a quantitative test of our diffusion equation solutions we consider ground-level concentrations, calculated for the $\beta = 0$ profile specified above, with $\hat{\epsilon} = 0$ (equation (2.12*a*)), and for the $\beta = 1$ profile, with $\hat{\epsilon} = 0$ (equation (2.16*a*)), and with $\hat{\epsilon} = 1$ (equation (2.21)).

We have chosen to focus on ground-level concentrations for the following two reasons:

(i) near the surface the timescale of velocity fluctuations becomes small so that a particle's velocity can be considered independent of the velocity imparted on leaving the source, as is implicitly assumed in all diffusion-equation calculations;

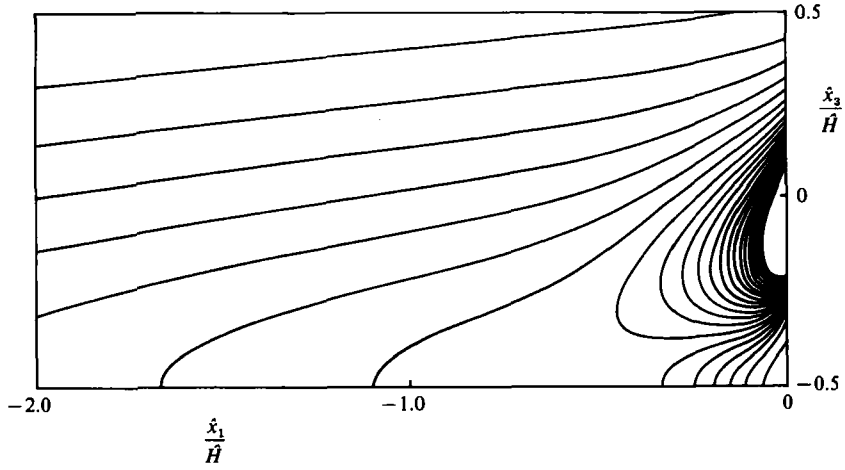

FIGURE 5. Concentration isopleths $\chi(\hat{x}_1, \hat{x}_3)$ for a line source in a reversing uniform shear flow.

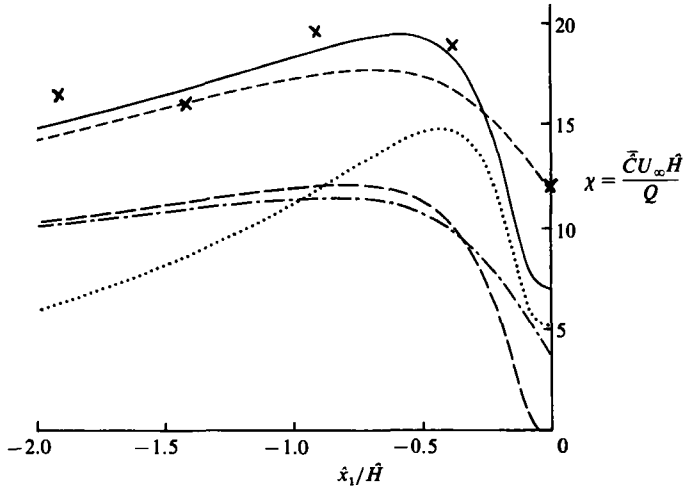

FIGURE 6. Ground-level concentrations for various diffusion approximations. ×, experiment (Quante & Etheridge 1984). 1. — — —, uniform non-reversing flow without streamwise diffusion ($\hat{\epsilon} \equiv 0$); 2. —·—·—·, uniform non-reversing flow with streamwise diffusion ($\hat{\epsilon} \equiv 1$); 3. ——, equation (2.16a) ($z = -h$) i.e. $\beta = 1$, $\hat{\epsilon} = 0$; 4. – – – – –, equation (2.21) ($z = -h$) i.e. $\beta = 1$, $\hat{\epsilon} = 1$; 5. · · · · ·, equation (2.12a) ($z = -h$) i.e. $\beta = 0$, $\hat{\epsilon} = 0$.

(ii) ground-level or surface concentrations are often the quantities of greatest interest in practical applications, such as deposition, heat exchange and air pollution.

We have also considered the ground-level concentration resulting when the backflow of $-0.1\ U_\infty$ in the $\beta = 0$ model is extended to $z = \infty$, rather than reversing at $z = 0$. Standard solutions exist for this problem with and without horizontal diffusivity (see e.g. Csanady 1973). Both these solutions are presented along with our three new solutions in figure 6 in comparison with the experimental points of Quante & Etheridge (unpublished observations). The comparison is quite revealing.

In the first place the diffusion-equation models which do *not* incorporate flow reversal give the poorest results (curves 1 and 2), underestimating the magnitude of the concentration maximum by 40 %. Of the other models, the $\beta = 1$ models (curves

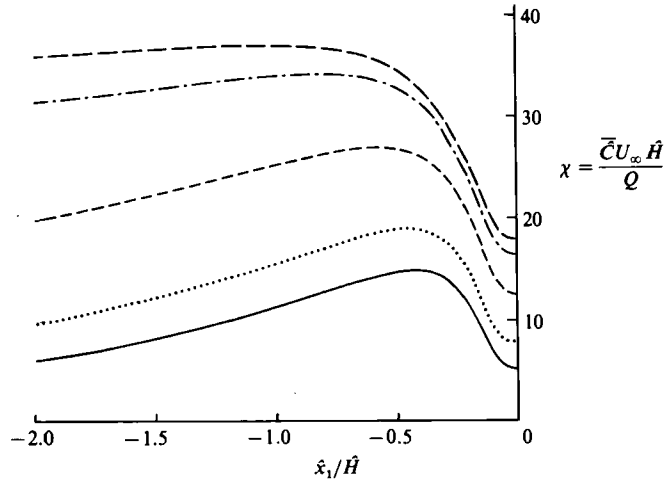

FIGURE 7. Ground-level concentrations obtained from (2.12a) with varying velocity in the upper layer. ————, $U_2/U_1 = 0.1$; —·—·—, $U_2/U_1 = 0.4$; – – – –, $U_2/U_1 = 1.0$; ·····, $U_2/U_1 = 4.0$; ——, $U_2/U_1 = 10.0$.

3 and 4) appear best, predicting fairly accurately both the position and the magnitude of the maximum ground-level concentration, whether or not horizontal diffusivity is incorporated. For the $\beta = 0$ case (curve 5) the maximum ground-level concentration is once more under-predicted, this time by 25%; in addition this maximum is predicted too near the source. It might be suggested that the under-prediction occurring for this latter case results from the associated over-prediction of the flow in the upper layer (see figure 4). However a further calculation in which the value of U_2 in the $\beta = 0$ model is reduced arbitrarily from U_∞ to 0.4 U_∞ (see below and figure 7), while yielding a much improved estimate of the value of the maximum of ground-level concentration, shows little improvement in the associated estimate of its streamwise position.

We conclude that:

(i) the models with reversing mean-flow profiles predict the ground-level concentration better than do those with unidirectional mean flow;

(ii) of the reversing profiles considered, the uniform shear (which profile is the closer to the real flow in the reversed layer) appears to be a better model than the step profile;

(iii) equation (2.4) may indeed prove useful for the estimation of surface concentrations in two-dimensional recirculating wakes for which the ratio of horizontal to vertical lengthscales is sufficiently large.

Thus our assumptions (i) and (ii) made in §2 appear to be acceptable, although it might be noted that the mathematical condition $\kappa_e \hat{L}/U_0 \hat{H}^2 \gg 1$, shown in §1 to be required for (ii) to hold in general, is not strictly satisfied; in our case

$$\frac{\kappa_e \hat{L}}{U_0 \hat{H}^2} \approx 1.$$

On this basis it seems worthwhile to use our diffusion-equation model with other parameter settings in order to probe the sensitivity of the dispersion process to these parameters.

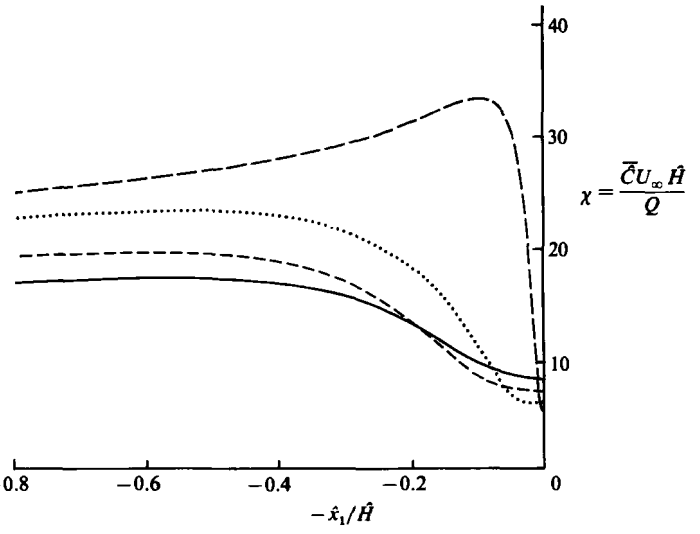

FIGURE 8. Ground-level concentrations obtained from (2.16*a*) for various source heights. ————, $h_s/h = 0.2$; · · · · ·, $h_s/h = 0.5$; – – – –, $h_s/h = 0.8$; ——, $h_s/h = 1.0$.

First we consider the effect of varying $U_2/U_1 (\equiv \tan^2\phi)$ in the $\beta = 0$ model. Figure 7 reveals that ground-level concentration is in fact a monotonically *decreasing* function of this parameter, as was suggested above: the effect of an increase in velocity in the upper layer is to remove contaminant more efficiently from the lower layer. We note that as $U_2/U_1 \to 0$ the ground-level concentration tends to reach a plateau at around $x = 40$, i.e. $\bar{\hat{C}} = 2Q/U_1\hat{h}$ for $\hat{x}_1 \geqslant 0.07$. The reason for this is discussed in the analysis of §4 below.

In order to answer our question (i) of §1 we consider the dependence of ground-level concentration on source height. This dependence has been studied, using the $\beta = 1$ model, by varying the assumed source height $h_s \equiv (h - z_0)$. Figure 8 shows the conclusions as plots of ground-level concentration for various values of the parameter h_s/h. (Note: the source position depicted in figure 6 corresponds to $h_s/h = 0.8$). Two trends are evident:

(i) lower source heights produce higher ground-level concentrations in the far field but lower ground-level concentrations in the vicinity of the source;

(ii) lowering the source height tends to bring the position of the maximum ground-level concentration closer to the source region.

The reason for the counter-intuitive tendency for the ground-level concentration immediately below the source to decrease as the source height is decreased is that, in the absence of longitudinal diffusion, this concentration results solely from recirculated contributions. A lowering of the source height causes contaminant to take longer to escape from the reversed layer; recirculation consequently becomes less efficient.

The two trends are displayed more clearly in figure 9 where χ_m, the maximum ground-level concentration and $\hat{x}_m$, the streamwise distance from the source at which this occurs are plotted as functions of h_s/h. We see that in fact for $h_s/h \gtrsim 0.75$ $\hat{x}_m$ starts to decrease again, contrary to the apparent trend evident in figure 8. This is a consequence of the counterflow in $z > 0$ making itself increasingly felt.

From the form of this graph some useful conclusions can be made of a rule-of-thumb

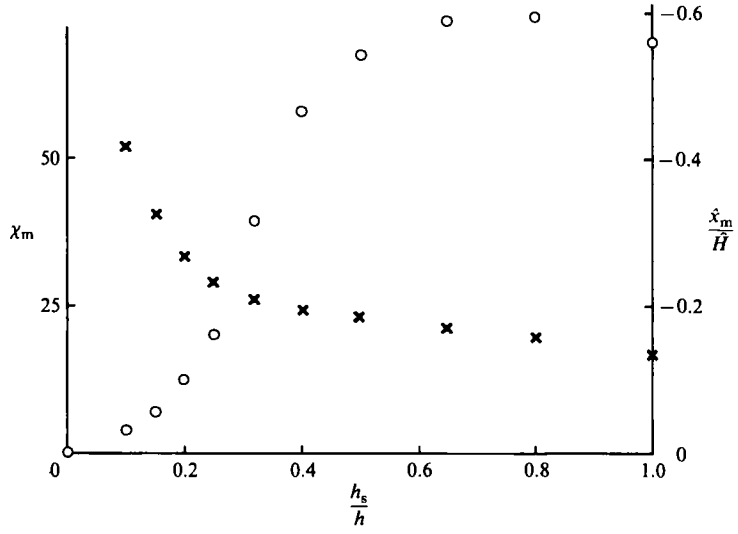

FIGURE 9. Variation of maximum ground-level concentration (χ_m) and its streamwise location ($\hat{x}_m$) obtained from (2.16a) for various source-heights. ×, χ_m (left-hand scale); ○, $\hat{x}_m/\hat{H}$ (right-hand scale).

type. Firstly we see that for $h_s/h \geqslant 0.5$, χ_m and $\hat{x}_m$ are roughly constant at around 20 and 0.6 $\hat{H}$ respectively. In terms of dimensional parameters, we therefore suggest the estimates

$$\bar{C}_m \simeq \frac{(1.7-2.3)Q}{\theta \hat{h}^2}; \quad \hat{x}_m \simeq 0.12\frac{\theta \hat{h}^3}{\kappa} \tag{3.1}$$

where θ denotes the mean shear in the reversed layer under consideration.

Secondly, for $h_s/h \lesssim 0.3$ a sharp rise in χ_m is evident; the suggestion is that for sources in the lowest one-third of the reversed layer, high peaks of ground-level concentration can be expected.† Location of sources in this lower region should thus be avoided in applications involving sources of pollution.

In order to probe the sensitivity of mean concentrations to turbulence levels in response to question (iv) in §1, we consider the effect of varying diffusivity, focusing first on streamwise diffusion. Important as this is in determining correctly the ground-level concentration below the source without recirculation (compare curves 1 and 2 and curves 3 and 4 in figure 6), it is found to have less effect on the magnitude or the position of the maximum ground-level concentration except when h_s/h becomes small ($\lesssim 0.3$).

Also, considering the form of our diffusion equation *without* streamwise diffusion ($\hat{\epsilon} = 0$), we note that the magnitude of the diffusivity does not itself affect the calculation except in the non-dimensionalization of the streamwise coordinate, $\hat{x}_1$. This leads us to the general conclusion that turbulence levels do *not* have a critical effect on the maximum ground-level concentration, but influence mainly just the position at which this occurs. In particular, the concentration profile at $\hat{x}_1 = 0$ is completely independent of κ.

† It should be remembered that near-source effects are poorly modelled by the diffusion equation so that the peak ground-level concentrations become unreliable for very low-level releases. Nevertheless from more detailed calculations with low-level sources Turfus (1985) has concluded that strong peaks of concentration are to be expected.

4. Asymptotic analysis

We have shown how our diffusion-equation solutions from §2 can be used to obtain numerical estimates of ground-level and other concentrations. However, it is also possible, by asymptotic analysis of our solutions, to draw some general conclusions about the structure of the concentration field established in a recirculating flow region. We focus on regions far from the source since that is where the diffusion-equation approximation is expected to have greatest validity.

We start with the expression (2.12*a*), although similar results can be drawn from the more general solution (A 9*a*). Clearly as x becomes large and negative within the lower layer, $C(x, z)$ becomes dominated by the $n = 0$ mode. Thus

$$C(x,z) \sim \frac{2}{h} \cos\left\{\frac{\phi(h-z_0)}{h}\right\} \cos\left\{\frac{\phi(h+z)}{h}\right\} e^{(\phi/h)^2 x} \quad \text{as } x \to -\infty,\ z < 0. \tag{4.1}$$

A similar result holds for $z > 0$. The exponential decay with x reflects the fact that even though the maximum of ground-level concentration occurs to the left of the source position, ultimately all the contaminant leaves the backward-flowing layer and is discharged (at $+\infty$) to the right. Of course in a real recirculating flow the backward layer does not extend to $-\infty$ but is deflected upwards after a finite length to recombine with the 'upper layer'. The effect is probably not dissimilar from our simple model.

What is of more interest to us, however, is the limit of (4.1) as $x \to -\infty$ *but* with $xU_2/U_1 \to 0$, i.e. $x\phi^2 \to 0$. Clearly in this case

$$C(x,z) \sim \frac{2}{h}. \tag{4.2a}$$

From our calculations in §3 where we saw (figure 7) that $C(x, z = -h)$ increases monotonically with U_1/U_2, we conclude that this value of $2/h$ is an asymptotic upper limit. It is interesting to compare this solution with that which would be obtained were the (almost) stagnant layer for $z > 0$ replaced by a rigid non-absorbing boundary at $z = 0$. Clearly for this case $\hat{C}(\hat{x}_1, \hat{x}_3) \sim Q/U_1\hat{h}$ or in non-dimensional terms

$$C(x,z) \sim \frac{1}{h}, \tag{4.2b}$$

exactly half the result (4.2*a*). In fact it can be shown that the formal limit of (2.12*a*) as $\phi \to 0$ is precisely the solution of the 'rigid-lid' problem $+1/h$. The latter term represents a uniform concentration in the lower layer to the *right* of the source.

With this result we can explain the trend observed in figure 7 as $U_2/U_1 \to 0$ and pointed out in §3. For with $h = 0.5$ and $U_1 = 0.1\ U_\infty$, (4.2*a*) implies $\chi \sim 40$ as $x \to -\infty$ and (4.2*b*) implies $\chi \sim 20$ at $x = 0$ (since $\chi \sim CU_\infty/U_1$ for the case $\beta = 0$). Figure 7 indeed appears to be consistent with both these limits. We are thus led to the very useful upper limit that for a source strength Q in a layer of depth $\hat{h}$ in which the mean flow is given by $\overline{U}$, the effect of recirculation is at worst to increase the concentration by an amount $Q/\overline{U}\hat{h}$.

If we consider the same limit applied to (A 9) we find that the concentration of recirculated contaminant is $1/h^{1+\beta}$ or in dimensional terms $\overline{\hat{C}} = Q/(1+\beta)\langle\overline{u}_1\rangle\hat{h}$ where $\langle\overline{u}_1\rangle$ is the mean flow averaged across the layer. Clearly $\beta = 0$ is the worst case of this so that our stated upper limit is valid not just for uniform profiles but for all power-law profiles of physical interest ($\beta \geqslant 0$).

Thus assuming again that our supposed negative answer to question (iii) (in §1) is correct, we can conclude in response to the remaining question (ii) that the maximum possible recirculated flux is equal to precisely the source rate. However it seems safe to further conclude from the present calculations that for most flow situations which are of practical interest and for which also $\hat{L} \gg \hat{H}$ (as in this case), the flux is unlikely to exceed about 50% of this figure.

Considering instead the limit of large and *positive* x, we can obtain results by expanding (2.14); the corresponding results for power-law profiles are in this case not so readily obtained.

We note first that for $z < 0$, in the limit $x/h^2 \to \infty$, $(x/h^2)(U_2/U_1) \to \infty$, the term

$$\frac{\cosh(u(h+z))\cosh(u(h-z_0))\sin 2\phi}{\cosh(2uh)+\cos 2\phi} \sim \cot\phi\{1-u^2(h^2\cot^2\phi + h(z_0+|z|)-\tfrac{1}{2}(z_0^2+|z|^2)\},$$

so that the integral (2.14a) can be expanded as

$$C(x,z) \sim \frac{2}{(4\pi U_2 x/U_1)^{\frac{1}{2}}}\left\{1-\frac{1}{2x}\left(\frac{h^2U_1}{U_2}+h(z_0+|z|)-\tfrac{1}{2}(z_0^2+z^2)\right)\right\}. \tag{4.3a}$$

The first term is just the term which would arise a distance x downstream of a point source on a rigid boundary $z = 0$ with $\bar{u}_1 = U_2$ everywhere; the effect of the backflow is to introduce a small negative correction $= O(1/x^{\frac{3}{2}})$. There is an associated backward flux of

$$F_- \sim \frac{-2U_1 h}{(4\pi U_2 x/U_1)^{\frac{1}{2}}}\left\{1-\frac{1}{2x}\left(h^2\left(\frac{U_1}{U_2}+\frac{1}{3}\right)+hz_0-\tfrac{1}{2}z_0^2\right)\right\}. \tag{4.3b}$$

Also relevant to our previous consideration of $U_2/U_1 \to 0$ for $x \ll -1$ is the corresponding limit for $x > 0$, $z < 0$, i.e.

$$\frac{x}{h^2} \to \infty; \quad \frac{U_2 x}{U_1 h^2} \to 0,$$

corresponding to downstream locations for which the distribution in the lower layer has reached its far-field form, but for which that in the upper layer has not. In this case we must alter our binomial expansion for $[\cosh(2uh)-\cos 2\phi]^{-1}$ and approximate

$$\frac{\cosh(u(h+z))\cosh(u(h-z_0))\sin 2\phi}{\cosh(2uh)-\cos 2\phi} \sim \frac{\sin\phi}{u^2h^2+\sin^2\phi},$$

so that from (2.14a),

$$C(x,z) \sim \frac{1}{h}\left\{1-\frac{2}{h}\left(\frac{U_2 x}{U_1 \pi}\right)^{\frac{1}{2}}\right\}. \tag{4.4}$$

We see that the leading-order solution here is the $1/h$ term deduced from the analysis for $x < 0$.

Finally for $z > 0$ with

$$\frac{x}{h^2} \to \infty; \quad \frac{xU_2}{h^2U_1} \to \infty; \quad \frac{hz}{2x} \to 0,$$

we find

$$C(x,z) \sim \frac{2\,\mathrm{e}^{-U_2 z^2/4U_1 x}}{(4\pi u_2 x/u_1)^{\frac{1}{2}}}\left\{1+\frac{1}{2x}\left[hz+\left(\frac{U_2 z^2}{2U_1 x}-1\right)\left(\frac{h^2U_1}{U_2}+hz_0-\tfrac{1}{2}z_0^2\right)\right]\right\}. \tag{4.5}$$

It can be shown (by calculating higher terms in this series) that the integrated flux $\int_0^\infty U_2 C(x,z)\,\mathrm{d}z$ in the upper layer satisfies $F_+ \sim 1 - F_-$ to the accuracy to which F_-

has been calculated in (4.3*b*). We note also from the form of this expansion that the maximum of $C(x,z)$ for fixed (large enough) x occurs at a height $z \sim hU_1/U_2$ *above* the reversed layer, rather than on the surface as occurs in the non-reversing case. This is because in the present case the establishment of a maximum of concentration at the wall is prevented by the continual dilution of the contaminant in the reversed-flow layer by cleaner fluid arriving from the right.

For values of x which are not $\gg h^2$ and values of z which are not small compared with x/h, an asymptotic expansion of $C(x,z)$ as a perturbation about a point source solution is *not* possible; we conclude that in such cases the influence of the backward-flowing layer on the spreading of the plume is not small.

5. Extension to point-source

In this section we consider the possible application of our diffusion-equation analysis to point sources in recirculating flows. The equation

$$u(z)\,C_x = C_{yy} + C_{zz} + \delta(x)\,\delta(y)\,\delta(z+z_0), \tag{5.1}$$

where

$$u(z) := -|z|^\beta \quad (-h \leqslant z \leqslant 0),$$

$$:= \Gamma z^\beta \quad (z > 0),$$

with $C \to 0$ as $(x^2+y^2+z^2)^{\frac{1}{2}} \to \infty$,

and $C_z(z=-h) = 0$,

does not appear to be soluble analytically for any value of β. However, we follow the expedient of Smith (1957) who approximated the lateral diffusion by assuming it can be described by

$$C(x,y,z) = \frac{C_0(x,z)\,\mathrm{e}^{-y^2/2\sigma_y^2(x,z)}}{(2\pi\sigma_y^2(x,z))^{\frac{1}{2}}} \tag{5.2}$$

where $\sigma_y^2(x,z)$ is a specified lateral spread and $C_0(x,z)$ is the line-source solution to the diffusion equation. Smith (1957) shows that $\sigma_y^2(x,z)$ can be calculated exactly by multiplying (5.1) by y^2 and integrating with respect to y from $-\infty$ to ∞ to obtain the following equation for

$$C_2(x,z) = \int_{-\infty}^{\infty} y^2 C(x,y,z)\,\mathrm{d}y:$$

$$u(z)\,C_{2x} - C_{2zz} = 2C_0(x,z) \quad (-h \leqslant z). \tag{5.3}$$

Clearly then, in terms of $C_2(x,z)$,

$$\sigma_y^2(x,z) = \frac{C_2(x,z)}{C_0(x,z)}. \tag{5.4}$$

Equation (5.3) has been solved in the region $x < 0$ for the $\bar{u}$ profile with $\beta = 1$, $\Gamma = 1$, for which $C_0(x,z)$ is given by (2.16). The solution is obtained fairly straightforwardly by noting that $C_0(x,z)$ is a Green function solution for the operator on the left-hand side of (5.3). After some algebra the solution can be written in the form

$$C_2(x,z) = 18 \sum_{n=1}^{\infty} \frac{\mathrm{e}^{(a_n'/h)^3 x}}{\mathrm{Ai}(-a_n')^2} \left\{ |x| \left(\frac{a_n'}{h}\right)^3 \frac{\mathrm{Ai}(a_n' z/h)\,\mathrm{Ai}(-a_n' z_0/h)}{(a_n')^2\,\mathrm{Ai}(-a_n')^2} \int_{-a_n'}^{\infty} \mathrm{Ai}(u)^2\,\mathrm{d}u \right.$$

$$\left. + \int_0^{\infty} \frac{u\,\mathrm{d}u\,D_n(u)[\mathrm{Ai}(-a_n' z_0/h)\,M(u,z) - \mathrm{Ai}(a_n' z/h)\,M(u_1,-z_0)]}{[u^3 + (a_n'/h)^3][\mathrm{Ai}'(uh)^2 + \mathrm{Bi}'(uh)^2]} \right\} \quad (x < 0), \tag{5.5}$$

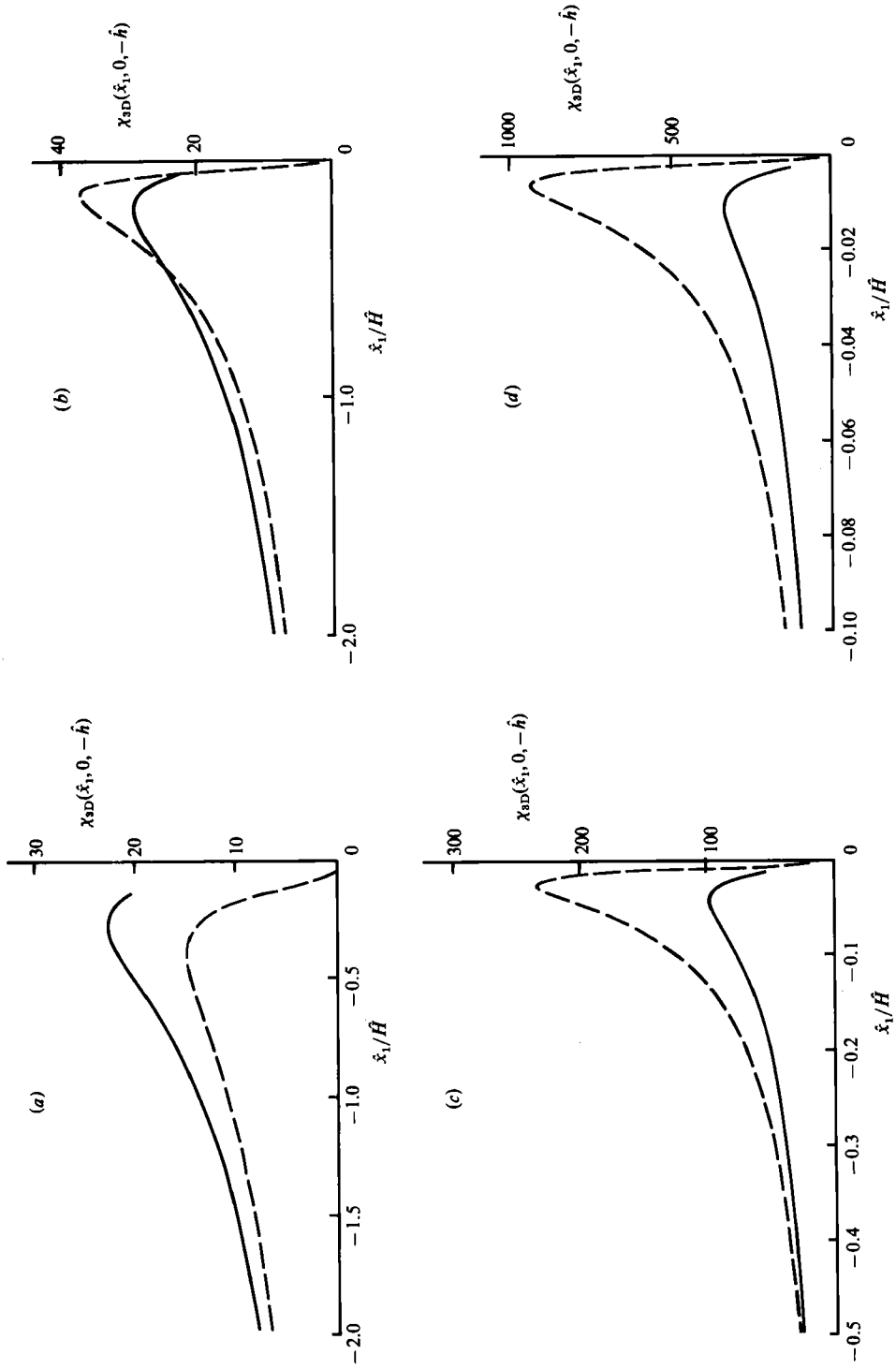

FIGURE 10. Estimates of ground-level concentration for various source heights (h_s/h), with point source. (*a*) $h_s/h = 0.8$; (*b*) $h_s/h = 0.5$; (*c*) $h_s/h = 0.2$; (*d*) $h_s/h = 0.1$. ——, equations (5.2)–(5.5) for uniform reversing shear flow; — — —, equation (5.6) derived for uniform non-reversing flow.

where we have used the notation

$$M(u,z) := \mathrm{Ai}(-uz)\,\mathrm{Bi}'(uh) - \mathrm{Bi}(-uz)\,\mathrm{Ai}'(uh),$$

and

$$D_n(u) := \int_0^\infty M(u,\zeta)\,\mathrm{Ai}\left(\frac{a_n'\zeta}{h}\right)\mathrm{d}\zeta.$$

The second integral is a little involved but fortunately gives a negligible contribution compared with the first expression and so can be ignored except for the smallest values of $|x|$.

This expression has been evaluated for the case $z=-h$ and used in conjunction with (5.2) and (5.4) to generate estimates of the centreline ground-level concentration $C(x,0,-h)$. These concentrations are plotted in terms of the standardized variable $\chi_{3D}=\bar{C}U_\infty \hat{H}^2/Q$ using dimensional variables $\hat{x}_1$ and $\hat{x}_3$ in figure 10. Also shown is the related exact solution

$$\chi_{3D}(\hat{x}_1,0,-\hat{h}) = \frac{U_\infty \hat{H}^2}{\kappa}\left(\frac{1}{4\pi|\hat{x}_1|}\right)\exp\left\{\frac{-\frac{1}{2}\theta\hat{h}(\hat{h}-\hat{x}_{30})^2}{4\kappa|\hat{x}_1|}\right\}, \tag{5.6}$$

obtained by using a uniform profile $\bar{u}_1(\hat{x}_3) = -\frac{1}{2}\theta\hat{h}$ in (5.1). (Note that the coordinate scales vary for the different graphs.)

It is observed that for high source heights the reversing shear profile results in higher ground-level concentrations than the uniform profile over a substantial range (for large enough $|x|$ it must always be smaller). As the source nears the surface, however, the uniform-profile calculation begins to predict the larger surface concentrations.

Consideration of the limit of small source height ($h_s/h\to 0$) is particularly useful. We note first that the flow at ground level in the reversing case is exactly twice that of the uniform one. Furthermore as $h_s/h\to 0$, the peak ground-level concentration for the reversing case must become independent of the shear and reversal, depending only on the flow speed at ground level. From this we conclude that the ratio of the peak ground-level concentrations for the reversing and uniform profiles respectively must tend to a limit of 0.5 as $h_s/h\to 0$. Inspection of figure 10(*c*, *d*), however, reveals that the calculated reversed flow ground-level concentrations drop to much less than half the corresponding uniform-flow values; indeed by $h_s/h = 0.1$ the ratio is as low as $\frac{1}{3}$.

We offer an explanation of this failing in our calculation, based on an idea discussed by Csanady (1983). He suggested that concentrations near the source should be thought of as being made up of two contributions: a primary component $C^{(1)}(\boldsymbol{x})$ resulting from direct advection from the source, and a background component $C^{(2)}(\boldsymbol{x})$, resulting from recirculated contaminant returning to the source region. In general, these two contributions will have quite distinct values of $\sigma_y^2(\boldsymbol{x})$, that of the former being considerably smaller. So instead of (5.2) a more realistic description of the lateral diffusion will be obtained by supposing

$$C(x,y,z) = C^{(1)}(\boldsymbol{x}) + C^{(2)}(\boldsymbol{x}) = \frac{C_0^{(1)}(x,z)\exp\left\{\dfrac{-y^2}{2\sigma_y^{(1)2}}\right\}}{(2\pi)^{\frac{1}{2}}\sigma_y^{(1)}(x,z)} + \frac{C_0^{(2)}(x,z)\exp\left\{\dfrac{-y^2}{2\sigma_y^{(2)2}}\right\}}{(2\pi)^{\frac{1}{2}}\sigma_y^{(1)}(x,z)}. \tag{5.7}$$

in obvious notation. This yields a centreline ground-level concentration of

$$\begin{aligned} C(x,0,-h) &= \frac{C_0^{(1)}(x,-h)}{(2\pi)^{\frac{1}{2}}\sigma_y^{(1)}(x,-h)} + \frac{C_0^{(2)}(x,-h)}{(2\pi)^{\frac{1}{2}}\sigma_y^{(2)}(x,-h)}, \\ &\sim \frac{C_0^{(1)}(x,-h)}{(2\pi)^{\frac{1}{2}}\sigma_y^{(1)}(x,-h)} \quad \text{as } h_s/h\to 0. \end{aligned} \tag{5.8}$$

Now we would expect for small source heights that $C_0(x,-h) \approx C_0^{(1)}(x,-h)$. However, in evaluating C_2 and hence σ_y^2 we cannot similarly ignore $C_2^{(2)}$ as being small compared with $C_2^{(1)}$. Hence we expect

$$\sigma_y^2(x,-h) := \frac{C_2(x,-h)}{C_0(x,-h)} \approx \frac{C_2(x,-h)}{C_0^{(1)}(x,-h)} > \frac{C_2^{(1)}(x,-h)}{C_0^{(1)}(x,-h)} = \sigma_y^{(1)2}(x,-h),$$

i.e. (5.2) will be an underestimate of the more accurate estimate (5.8) of the asymptotic limit of peak ground-level concentration as $h_s/h \to 0$. (An example of this is given by Castro & Snyder (1982) from their wind-tunnel experiment. Their figure 22 shows clearly that for small h_s/h the lateral profile of ground-level concentration takes on a 'double Gaussian' form with a narrow peak superimposed on a broad one. Matching such a profile by a single Gaussian one is bound to underestimate the centreline concentration.)

It is our suggestion that a better estimate of centreline ground-level concentration for the lower source heights ($h_s/h \leqslant 0.3$, say) will be obtained by the more heuristic procedure of using in (5.2) a $\sigma_y^2(x,z)$ value calculated for a point source in the uniform flow given by

$$\langle \bar{u}_1 \rangle = \frac{1}{\hat{h}-\hat{x}_{30}} \int_{-\hat{h}}^{-\hat{x}_{30}} \bar{u}_1(\hat{x}_3)\,\mathrm{d}\hat{x}_3.$$

Extensive numerical computation would probably be necessary to confirm whether such a procedure is appropriate in general. Certainly it will yield the correct asymptotic limit (5.8).

An alternative method, suitable if the source is near the stagnation point $z = 0$, is to use the $\sigma_y^2(x,z)$ results of Smith (1957) for a ground-level source, but evaluated at $z = +h$, thinking of our reversed layer as his problem upside down. If the shear in the layer is uniform to a good approximation, then the result for $\sigma_y^2(x,z)$ is particularly simple, being given by an incomplete γ function (see his equations (4.3), (4.4), (4.25) and (4.26)).

If, however, we suppose that our first calculation is appropriate for values of $h_s \geqslant 0.5$, computation shows that both the re-nondimensionalized maximum ground-level concentration $\chi_{3\mathrm{Dm}} = U_\infty C_{3\mathrm{Dm}}/\hat{H}\theta$ and its position $\hat{x}_{3\mathrm{Dm}} := x\theta\hat{H}^3/\kappa$ are fairly constant over this range, and given by

$$\chi_{3\mathrm{Dm}} \approx 20\text{–}30; \quad \chi_{3\mathrm{Dm}} \approx (0.2\text{–}0.3)\,\hat{H}.$$

For the particular case of $h_s/h = 0.8$, the precise value $\chi_{3\mathrm{Dm}} = 22$ agrees well with the value of 24 computed by Turfus (1985) but the value $\hat{x}_{3\mathrm{Dm}} = 0.29\hat{H}$ is an underestimate of the value $0.6\hat{H}$ found there, probably reflecting the inadequate representation of near-source diffusion implicit in our diffusion equation.

Expressing our result once more in dimensional notation, we predict that for a source at height $\hat{h}-\hat{x}_{30} \geqslant \frac{1}{2}\hat{h}$ in a reversed layer in which the diffusivity is κ and the velocity given by $\bar{u}_1(\hat{x}_3) = \theta\hat{x}_3$, $\hat{x}_3 \in [-\hat{h}, 0]$:

$$\bar{C}_{3\mathrm{Dm}} \approx \frac{(1\text{–}1.5)\,Q}{\theta\hat{h}^3}; \quad \hat{x}_{3\mathrm{Dm}} \approx \frac{(0.04\text{–}0.06)\,\hat{h}^3\theta}{\kappa}. \tag{5.9}$$

Finally, we make a rough comparison with the result of Wilson & Britter (1982) for the concentration due to a source on the back wall of a surface-mounted cube of height $\hat{H}$ where the upstream flow velocity is U_∞. For such a flow configuration, three-dimensional effects in the form of streamwise and axial vortices are known to be important and, in addition, $\hat{L}/\hat{H} \approx 1.5$ so neither of our assumptions of two-

dimensionality nor of $\hat{L} \gg \hat{H}$ hold. It will be seen, nevertheless, that useful results appear to be obtained. Based on theory and a survey of wind-tunnel and field studies, Wilson & Britter suggest

$$\chi_{3D} \approx (1\text{–}5).$$

If we estimate $\hat{h} \approx \hat{H}$ and $\theta \approx U_R/\hat{H}$ where U_R is the maximum ground-level backflow velocity in such a situation (typically $0.2U_\infty$, see Robins & Castro 1977), our model yields

$$\chi_{3Dm} \approx (5\text{–}7.5),$$

which is quite compatible with Wilson & Britter's (1982) suggestion. More recent evidence from field studies by Jones & Griffiths (1984) suggests

$$\chi_{3D} \approx (2.7\text{–}6.5).$$

The level of agreement between these experimental results and our simple predictions based on knowledge only of the shear and of the width of the reversed-flow layer is rather surprising. Our original assumption that reattachment effects can be neglected in favour of correct modelling of the local mean flow, for sources located well within a recirculating flow, appears to be again supported.

6. Conclusions

In this last section an attempt is made to bring together some of the conclusions of the preceding analysis. However, it is worthwhile reminding ourselves beforehand of the assumptions subject to which that analysis was carried out. These were:

(i) that diffusion can be described by the diffusion equation (2.1), and further that κ_{ij} can be modelled with all diagonal components set equal to constants and all non-diagonal components set equal to zero;

(ii) that mean vertical motions can be neglected for sources in the centre of the recirculating wake (and consequently that the effects of reattachment are negligible).

The justification for these assumptions is wholly *a posteriori*. In order to decide more generally when the second of these assumptions might be justifiable, detailed computations involving fully two-dimensional flows would be necessary. An investigation into the general applicability of the first assumption would be an extremely difficult and lengthy task.

Nevertheless it does appear, from our success in estimating ground-level concentrations in the vicinity of the source, that even if the above assumptions are not strictly valid for our problem, their adoption has not seriously prejudiced our results; support for our adopted procedure seems to be found even from the example of the fully three-dimensional flow behind the surface-mounted cube, for which assumption (ii) is obviously inapplicable. The reason why such success was found is not apparent. Some explanation might be offered in the case of the two-dimensional flow as to why the local as opposed to global mean flow is determinative of the mean ground-level concentration. For although the mean flow in this case is such that $\hat{L} \gg \hat{H}$, the instantaneous flow in the middle of the wake is known to be made up of vortex structures whose horizontal as well as vertical scale is $O(\hat{H})$ (Tani, Iuchi & Komada 1961). Thus the recirculation of contaminant can be considered to occur on a short horizontal lengthscale $O(\hat{H})$ rather than on the lengthscale $O(\hat{L})$. This argument, of course, does not apply to the three-dimensional flow problem considered, and the favourable result in that case may prove to have been more coincidental.

The results concerning ground-level concentrations are presented first; having been verified against experiment they are the most reliable conclusions. Further conclusions about the broad structure of the concentration field are then presented, subject to the supposition that the diffusion-equation solutions are applicable away from, as well as at, ground level. Finally, some suggestions are made about related problems which can be tackled by methods similar to those described above.

6.1. *Results for ground-level concentration*

Our analysis yields the interesting result that an upper limit to the flux of recirculated contaminant in a backward-flowing layer width $\hat{h}$ at the location of a line-source strength Q per unit length is Q. For most practical applications, however, a value of $\frac{1}{2}Q$ is unlikely to be exceeded. A reasonable first approximation to the concentration in the backward-flowing layer to the right of the source is then

$$\overline{C} \approx Q \Big/ \left(2 \int_{-\hat{h}}^{0} \overline{u}_1 \, \mathrm{d}\hat{x}_3 \right). \tag{6.1}$$

The concentration to the left of the source can in turn be estimated by adding to this the contribution resulting from a simple plume.

For a line-source located in the top half of the reversed-flow layer the maximum ground-level concentration and its streamwise location are as expressed in (3.1). The corresponding results for a point-source subject to the same conditions are expressed in (5.9). Cases involving sources in the lower half of the reversed-flow layer require more careful calculation, particularly cases involving point sources because of the associated difficulties, discussed in §5, of representing the lateral spread.

It has been found that longitudinal diffusion is important in determining the ground-level concentration immediately below the source (compare curves 3 and 4 of figure 6) but otherwise it has little effect on the ground-level concentration. This being the case, the major influence that the magnitude of the vertical diffusivity has on the ground-level concentration is in the scaling of the horizontal coordinate, i.e. if κ increases, the streamwise position of the maximum of ground-level concentration moves proportionally closer to the source but its magnitude remains fixed.

The fact that the uniform shear ($\beta = 1$), which is a better model of the real mean flow in the reversed-flow layer, furnishes better results than the step profile ($\beta = 0$), suggests that the correct modelling of the mean flow in the reversed layer may be critical in estimating ground-level concentrations.

It can be seen that, since concentration is inversely proportional to flow velocity, the effect of decreasing the speed in both layers proportionally is to increase all concentrations by the same proportion. However, when the velocity in the upper layer was decreased, with that in the lower layer held fixed, a monotonic increase in the ground-level concentration was observed. As the velocity in the upper layer tended to zero, an asymptotic ground-level-concentration profile was approached. Finally, the observed effect of lowering the source height was to increase the maximum of ground-level concentration and bring it closer to the source region; a tendency for the concentration immediately below the source simultaneously to decrease was explained by the absence of horizontal diffusion and would certainly not have been observed had horizontal diffusion been incorporated into the model.

6.2. *Structure of the concentration field*

For the purpose of discussing the general structure of the concentration field, this has been divided schematically into five regimes, as indicated in figure 11. These are dealt with separately below.

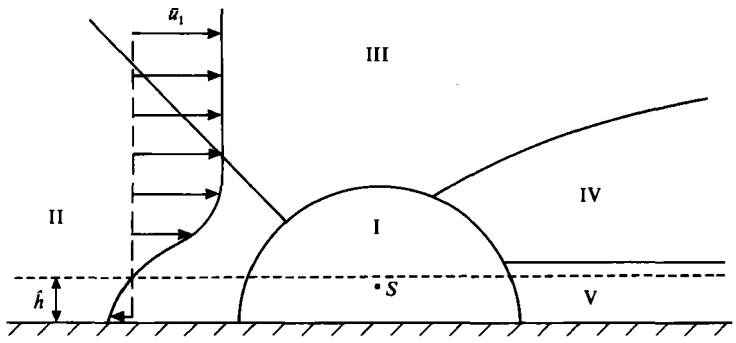

FIGURE 11. Five regimes of concentration field.

I. In the near-source region the concentration field has the character of a plume, which dips towards and then moves along the surface. The plume descent observed in figure 5 for the case of a uniform mean shear is much faster than would result from the influence of an image plume. This is because of a combination of two effects: firstly the tendency noted by Okubo & Karweit (1969) for the position of maximum concentration of a plume in a shear to shift in the direction of increasing velocity as one moves downstream; secondly, the tendency for a plume beneath a counter-flowing stream to be eroded at one side as contaminant is preferentially removed by the stream.

II. Further to the left of the source, there occurs an exponential decay of concentration with increasing $\hat{x}_1$. This decay occurs in a distance of $O(U_0\hat{h}^2/\kappa)$ where U_0 is a typical backflow velocity, $\hat{h}$ is the layer width and κ is an estimate of the effective vertical turbulent diffusivity. It should be noted that in practical applications, this exponential decay will in most cases be interrupted by the onset of vertical mean motion. Nevertheless, all contaminant must eventually be advected away to the right.

III. In the region above the source, away from the reversed layer, there occurs an exponential decay with height $\hat{x}_3$. From the form of (A 9*b*) this can be seen to occur in a distance of $O(\hat{h}/(\mu_1\Gamma^{\frac{1}{2}})^{1/\alpha})$ where α is as defined in the Appendix, i.e. $\alpha = 1+\frac{1}{2}\beta$, and μ_1 is the smallest root of (A 7) and so is a function of both β and Γ. Two special cases are of note: firstly, the limit as $\Gamma = U_2/U_1 \to 0$ for which decay occurs over a distance $O(\hat{h}/\Gamma^{1/(1+\beta)})$; secondly, the more practically interesting limit of $\Gamma = U_2/U_1 \to \infty$ for which decay occurs over a distance $O(\hat{h}/\Gamma^{1/(3+\beta)})$.

IV. To the right of the source but away from the surface, the concentration in the plume is approximately described by the solutions calculated by Smith (1957) for a ground-level source in a non-reversing shear flow, the effective origin in our case being $(\hat{x}_1, \hat{x}_3) = (0, 0)$.

V. In the region near the surface to the right of the source, a dilution of the concentration occurs due to the reverse flow returning low concentration fluid towards the source. Thus at no streamwise station to the right of the source is the concentration profile found to reach a maximum at the surface. Our calculations based on the case $\beta = 0$ suggest that the maximum will in fact tend to occur at a distance $O(\hat{h}U_1/U_2)$ above the reversed-flow layer.

6.3. *Related problems*

Finally, although not presented here, other solutions can be found, by similar techniques, for the following problems adapted from the one presently considered:

(i) absorbing boundary, by replacing the condition $\partial C/\partial z = 0$ by $C = 0$ on $z = -h$ (equation (2.7b));

(ii) source outside the reversed-flow region (note that the solutions (2.16) and (2.21) actually apply to sources inside *or* outside the reversing layer);

(iii) buoyant contaminant (well diluted) by adding the term $w\,\partial C/\partial z$ to the left-hand side of (2.6a, b), where $wU_1\hat{H}^\beta$ is a terminal rise (or fall) velocity for the contaminant particles;

(iv) a solution is presented by Turfus (1985) for a parabolic diffusivity profile with a non-zero value at ground-level in the case $\beta = 0$ (uniform-velocity profiles). This appears to be the only easily soluble case involving variable diffusivity.

The first two of these problems have solutions which are merely analogues of solutions described above; the third and fourth are less obvious and require some additional calculation. Only the last of these solutions has been calculated in detail by the author.

I would like to extent my thanks to my research supervisor, Dr J. C. R. Hunt, for his help in preparing this paper; also to Dr R. Smith for encouragement and advice about tackling the problem; and finally to the British Gas Corporation who funded the research through their Research Scholarship scheme.

Appendix: General solution for diffusion equation with counter-flowing mean flow profiles governed by power laws

We solve the problem given by (2.6) with boundary conditions given by (2.7). It is more convenient to express the solution with the notation

$$\beta = 2\alpha - 2; \quad \Gamma = \gamma^{2\alpha}.$$

We suppose only that $\alpha > 1$.

Taking a Fourier transform, and putting $\xi^2 = ik$, (2.6) becomes†

$$|z|^{2\alpha-2}\xi^2\tilde{C} + \tilde{C}_{zz} = \frac{-\delta(z+z_0)}{2\pi} \quad (-h \leqslant z \leqslant 0, \tag{A 1}$$

$$\gamma^{2\alpha} z^{2\alpha-2}\xi^2\tilde{C} - \tilde{C}_{zz} = 0 \quad (z > 0). \tag{A 2}$$

The solutions to (A 1) with right-hand side = 0 are linear multiples of

$$|z|^{\frac{1}{2}} J_{\frac{1}{2\alpha}}\left(\frac{\xi|z|^\alpha}{\alpha}\right); \quad |z|^{\frac{1}{2}} J_{-\frac{1}{2\alpha}}\left(\frac{\xi|z|^\alpha}{\alpha}\right)$$

(Bender & Orszag 1978 p. 573). The solution to (A 2) satisfying $\tilde{C} \to 0$ as $z \to \infty$ is a multiple of

$$z^{\frac{1}{2}} K_{\frac{1}{2\alpha}}\left(\frac{\xi[\gamma z]^\alpha}{\alpha}\right).$$

For the region $-z_0 < z < 0$ we need to form a solution which satisfies continuity of $\tilde{C}$ and $\partial\tilde{C}/\partial z$ with the solution for $z > 0$. By expanding the Bessel functions $J_{+(1/2\alpha)}$ and $K_{(1/2\alpha)}$ for small argument, we see the form of solution required is $|z|^{\frac{1}{2}} y_1^{(\alpha)}(\xi|z|^\alpha/\alpha)$ where

$$y_1^{(\alpha)}(u) := \gamma^{-\frac{1}{2}} J_{-\frac{1}{2\alpha}}(u) + \gamma^{\frac{1}{2}} J_{\frac{1}{2\alpha}}(u). \tag{A 3a}$$

† Here and elsewhere subscripts x, y and z denote partial derivatives with respect to these variables.

In order to preserve symmetry we define a second linearly independent solution applicable to $-h \leqslant z < -z_0$ by $|z|^{\frac{1}{2}} y_2^{(\alpha)}(\xi|z|^\alpha/\alpha)$ where

$$y_2^{(\alpha)}(u) = \gamma^{-\frac{1}{2}} J_{-\frac{1}{2\alpha}}(u) - \gamma^{\frac{1}{2}} J_{\frac{1}{2\alpha}}(u). \tag{A 3b}$$

We shall need the Wronskian of these two solutions; this can be seen to be:

$$W(|z|^{\frac{1}{2}} y_1^{(\alpha)}\left(\frac{\xi|z|^\alpha}{\alpha}\right), |z|^{\frac{1}{2}} y_2^{(\alpha)}\left(\frac{\xi|z|^\alpha}{\alpha}\right) = \frac{4\alpha}{\pi} \sin\left(\frac{\pi}{2\alpha}\right), \tag{A 4}$$

where

$$W(y_1, y_2) := y_1 \frac{\partial y_2}{\partial z} - y_2 \frac{\partial y_1}{\partial z}.$$

The solution for $-h \leqslant z < -z_0$, must have the form

$$|z|^{\frac{1}{2}} \left\{ y_2^{(\alpha)}\left(\frac{\xi|z|^\alpha}{\alpha}\right) - \theta(\xi)\, y_1^{(\alpha)}\left(\frac{\xi|z|^\alpha}{\alpha}\right) \right\},$$

where $\theta(\xi)$ is specified so that the solution satisfies $\partial \bar{C}/\partial z|_{z=-h} = 0$. That is, we must have

$$\theta(\xi) = \left. \frac{\partial/\partial u(u^{\frac{1}{2}} y_2^{(\alpha)}(\xi u^\alpha/\alpha))}{\partial/\partial u(u^{\frac{1}{2}} y_1^{(\alpha)}(\xi u^\alpha/\alpha))} \right|_{u=h}. \tag{A 5}$$

From (A 3)–(A 5) we can construct a Green function solution for $-h \leqslant z \leqslant 0$:

$$\bar{C}(k,z) = \frac{-|z|^{\frac{1}{2}} y_1^{(\alpha)}(\xi z_0^\alpha/\alpha)}{8\alpha \sin(\pi/2\alpha)} \left\{ y_2^{(\alpha)}\left(\frac{\xi|z|^\alpha}{a}\right) - \theta(x)\, y_1^{(\alpha)}\left(\frac{\xi|z|^\alpha}{a}\right) \right\} (-h \leqslant z < -z_0) \tag{A 6a}$$

$$= \frac{-|z|^{\frac{1}{2}} y_1^{(\alpha)}(\xi|z|^\alpha/\alpha)}{8\alpha \sin(\pi/2\alpha)} \left\{ y_2^{(\alpha)}\left(\frac{\xi z_0^\alpha}{\alpha}\right) - \theta(\xi)\, y_1^{(\alpha)}\left(\frac{\xi z_0^\alpha}{\alpha}\right) \right\} (-z_0 \leqslant z \leqslant 0). \tag{A 6b}$$

The solution for $z > 0$ matching onto (A 6*b*) is

$$\bar{C}(k,z) = \frac{-z^{\frac{1}{2}} K_{\frac{1}{2\alpha}}(\xi(\gamma z)^\alpha/\alpha)}{2\pi\, 2\alpha} \left\{ y_2^{(\alpha)}\left(\frac{\xi z_0^\alpha}{\alpha}\right) - \theta(\xi)\, y_1^{(\alpha)}\left(\frac{\xi z_0^\alpha}{\alpha}\right) \right\}. \tag{A 6c}$$

The expressions in (A 6) can be inverse transformed using (2.11). For $x < 0$, we use Cauchy's theorem to transform the k-integration path onto the contour C_1 depicted in figure 3.† The integral can then be evaluated as a sum of the residues at the poles on the imaginary k-axis. The poles occur when the denominator of $\theta(\xi)$ in (A 5) is zero, i.e. at $\xi = \alpha\mu_n/h^\alpha$ where $\{\mu_n : n = 1, 2, 3, \ldots\}$ is the set of all values of μ satisfying

$$\frac{\mathrm{d}}{\mathrm{d}\mu}(\mu^{1/2\alpha} y_1^{(\alpha)}(\mu)) = 0. \tag{A 7}$$

† We have assumed that $\theta(\xi)$ has no singularities in the region $\mathscr{D} = \{\xi : \arg\xi \in (0, \frac{1}{2}\pi) \cup (-\pi, 0)\}$. A proof of this assertion can be built up along the following lines. We note first that the real ξ axis is a Stokes' line for the function, $f(\xi) = \partial/\partial u(u^{\frac{1}{2}} y_1^{(\alpha)}(\xi u^\alpha/\alpha))|_{u=h}$; this function satisfies $|f(\xi)| \to \infty$ as $|\chi| \to \infty$ for $\xi \in \mathscr{D}$. Then all zeros of f in $\mathscr{D}$ must satisfy $|\xi| \arg\xi < R$, for some $R > 0$. Consider $f = \phi + i\psi$, where ϕ, ψ are real and harmonic since f is analytic away from 0. We see that since $\psi = 0$ on the real axis, the lines of $\phi = 0$ cut the real ξ-axis at right angles, at the zeros of f (denoted μ_n in the text). Any zero of f away from the real ξ-axis implies the existence of a $(\psi = 0)$-line cutting the $(\phi = 0)$-lines at right-angles: such lines must be constrained to go to ∞ within $\mathscr{D}$ or else pass through the real ξ-axis, neither of which is possible. For, since the μ_ns are unbounded, lines of $\psi = 0$ going to ∞ in $\mathscr{D}$ would imply unbounded zeros of f in $\mathscr{D}$, contradicting our previous assertion (unless the line asymptotes to the real ξ-axis which, from the asymptotic form of $f(\xi)$ can be shown not to happen); on the other hand, $(\psi = 0)$-lines in $\mathscr{D}$ cannot meet the real ξ-axis (except at the origin) because it is itself a $(\psi = 0)$-line and such lines cannot meet at a regular point of f.

We need

$$\lim_{\xi\to\frac{\mu_n\alpha}{h^\alpha}}(\xi-\mu_n\alpha/h^\alpha)\,\theta(\xi)=\frac{h^{\frac12}\partial/\partial u(u^{\frac12}y_2^{(\alpha)}(\xi u^\alpha/\alpha))}{h^\alpha\mu_n\,y_1^{(\alpha)}(\mu_n)}\Big|_{\substack{u=h\\ \xi=\alpha\mu_n/h^\alpha}} \tag{A 8}$$

where we have used (A 5), (A 7) and the fact that $|z|^\alpha y_1^{(\alpha)}(\xi|z|^\alpha)/\alpha$ satisfies (A 1) with the right-hand side = 0.

The solution for $-h\leqslant z<-z_0$, which by symmetry also holds for $-z_0<z\leqslant 0$, can then be written

$$C(x,z)=\sum_{n=1}^{\infty}-|z|^{\frac12}\left\{\frac{2\xi y_1^{(\alpha)}(\xi z_0^\alpha\,\alpha)\,y_1^{(\alpha)}(\xi|z|^\alpha/\alpha)\,\mathrm{e}^{\xi^2x}}{(4\alpha/\pi)\sin(\pi/2\alpha)}\right\}_{\xi=\mu_n\alpha/h^\alpha}\lim_{\xi\to\frac{\mu_n\alpha}{h^\alpha}}\left(\xi-\frac{\mu_n\alpha}{h^\alpha}\right)\theta(\xi).$$

From (A 8) and the fact that (from (A 4) and the definition of the μ_n)

$$h^{\frac12}y_1^{(\alpha)}(\mu_n)\left\{\frac{\mathrm{d}}{\mathrm{d}u}(u^{\frac12}y_2^{(\alpha)}(\xi u^\alpha/\alpha))\right\}_{\substack{u=h\\ \xi=\alpha\mu_n/h^\alpha}}=-\left(\frac{4\alpha}{\pi}\right)\sin\left(\frac{\pi}{2\alpha}\right),$$

we conclude:

$$C(x,z)=\frac{2\alpha|z|}{h^{2\alpha}}\sum_{n=1}^{\infty}\frac{y_1^{(\alpha)}(\mu_n(|z|/h)^\alpha)\,y_1^{(\alpha)}(\mu_n(z_0/h)^\alpha)\,\mathrm{e}^{(\alpha\mu_n/h^\alpha)^2x}}{y_1^{(\alpha)}(\mu_n)^2}\quad(x<0;\ -h\leqslant z\leqslant 0). \tag{A 9a}$$

Similarly from (A 6c)

$$C(x,z)=\frac{2\sin(\pi/2\alpha)}{h^{2\alpha}(\pi/2\alpha)}\sum_{n=1}^{\infty}\frac{K_{\frac12\alpha}(\mu_n(\gamma z/h)^\alpha)\,y_1^{(\alpha)}(\mu_n(z_0/h)^\alpha)\,\mathrm{e}^{(\alpha\mu_n/h^\alpha)^2x}}{y_1^{(\alpha)}(\mu_n)^2}\quad(x<0;z>0). \tag{A 9b}$$

On putting $\gamma=1$, $\alpha=\frac32$, these expressions can both be shown to reduce to (2.16a).

For the case $x>0$ we put $\xi=u\,\mathrm{e}^{\frac12\mathrm{i}\pi}$ in (A 6) and deform the k-integration path onto C_2 (see figure 3). For $-h<z<-z_0$, (A 6a) substituted into (2.11) yields

$$C(x,z)=2\,\mathrm{Re}\int_0^\infty\frac{2u\,\mathrm{d}u\,\mathrm{e}^{-u^2x}}{\mathrm{i}8\alpha\sin(\pi/2\alpha)}|z|^{\frac12}y_1^{(\alpha)}\left(\frac{\mathrm{i}uz_0^\alpha}{\alpha}\right)\left\{y_2^{(\alpha)}\left(\frac{\mathrm{i}u|z|^\alpha}{\alpha}\right)-\theta(\mathrm{i}u)\,y_1^{(\alpha)}\left(\frac{\mathrm{i}u|z|^\alpha}{\alpha}\right)\right\}.$$

The complex arguments of $y_2^{(\alpha)}(.)$ and $\theta(.)$ can be dealt with by noting

$$J_\nu(\mathrm{i}z)=\mathrm{e}^{\frac12\mathrm{i}\nu\pi}I_\nu(z),$$

(Bender & Orszag 1978 p. 572). Making this substitution, after some lengthy algebra and taking the real part, we obtain

$$C(x,z)=\int_0^\infty\frac{1}{\alpha}\frac{\mathrm{e}^{-u^2x}\,M_u(|z|,h)\,M_u(z_0,h)\,u\,\mathrm{d}u}{\left[\gamma f_+'(h;u)^2+2\cos\dfrac{\pi}{2\alpha}f_+'(h;u)f_-'(h;u)+\gamma^{-1}f_-'(h;u)^2\right]}, \tag{A 9c}$$

where we have used the notation:

$$f_\pm(h;u):=h^{\frac12}I_{\pm\frac{1}{2\alpha}}\left(\frac{uh^\alpha}{\alpha}\right);$$

$$M_u(z,h):=f_+(z;u)f_-'(h;u)-f_-(z;u)f_+'(h;u),$$

and $f'(.\,;u)$ denotes differentiation with respect to the first argument.

A similar expression holds for $x>0$, $z>0$.

REFERENCES

BENDER, C. M. & ORSZAG, S. A. 1978 *Advanced Mathematical Methods for Scientists and Engineers.* McGraw Hill.

CASTRO, I. P. & SNYDER, W. H. 1982 A wind-tunnel study of dispersion from sources downwind of three-dimensional hills. *Atmos. Env.* **16** (8), 1869–1887.

CORSSIN, S. 1974 Limitations of gradient transport models in random walks and in turbulence. International Symp. on Turbulent Diffusion in Environmental Pollution. *Adv. Geophys.* **18A**, 25–60.

CSANADY, G. T. 1973 *Turbulent Diffusion in the Environment.* Reidel.

CSANADY, G. T. 1983 Dispersal by randomly varying currents. *J. Fluid Mech.* **132**, 375–394.

ELRICK, D. E. 1962 Source functions for diffusion in a uniform shear flow. *Austral. J. Phys.* **115** (3), 283–287.

JONES, C. D. & GRIFFITHS, R. F. 1984 Full-scale experiments on dispersion around an isolated building using an ionised air tracer technique with very short averaging time. *Atmos. Env.* **18** (5), 903–916.

KAY, A. 1985 The effect of cross-stream depth variation upon contaminant dispersion in a vertically-well-mixed current. (To be published.)

LUDFORD, G. S. S. & ROBERTSON, R. A. 1973 Fully diffused regions. *SIAM J. Appl. Maths* **25**, 693–703.

OKUBO, A. & KARWEIT, M. J. 1969 Diffusion from a continuous source in a uniform shear flow. *Limnol. Oceanogr.* **14**, 514–520.

PEDLEY, T. J. 1980 *The Fluid Mechanics of Large Blood Vessels.* Cambridge University Press.

ROBINS, A. G. & CASTRO, I. P. 1977 A wind tunnel investigation of plume dispersion in the vicinity of a surface mounted cube. I. The flow field. *Atmos. Env.* **11**, 291–297.

SMITH, F. B. 1957 The diffusion of smoke from a continuous elevated point-source into a turbulent atmosphere. *J. Fluid Mech.* **2**, 49–76.

TANI, I., IUCHI, M. & KOMADA, H. 1961 Experimental investigation of flow separation associated with a step or groove. *Aeronautical Res. Inst. Univ. Tokyo, Rep.* no. 364.

TAYLOR, G. I. 1953 Dispersion of soluble matter in solvent flowing slowly through a tube. *Proc. R. Soc. Lond.* A **219**, 186–203.

TURFUS, C. 1985 Stochastic modelling of turbulent dispersion near surfaces. Ph.D. thesis, Dept. Applied Mathematics and Theoretical Physics, University of Cambridge.

WILSON, D. J. & BRITTER, R. E. 1982 Estimates of building surface concentrations from nearby point sources. *Atmos. Env.* **16** (11), 2631–2646.